6th International Congress of Serbian Society of Mechanics
Mountain Tara, Serbia, June 19-21, 2017

CALCULATION OF THE ACCELERATION FORCE COMPONENTS AND ROLL AND PITCH LINK ANGLES OF THE CFS AND SDT

Vladimir Kvrgić[1], Jelena Vidaković[1], Mihailo Lazarević[2], Goran Pavlović[1]

[1] Lola Institute, Kneza Viseslava 70a, 11030, Belgrade, Serbia
e-mail: vladimir.kvrgic@li.rs, jelena.vidakovic@li.rs, goran.pavlovic@li.rs
[2] Faculty of Mechanical Engineering,
The University of Belgrade, Kraljice Marije 16, 11120 Belgrade 35
e-mail: mlazarevic@mas.bg.ac.rs

Abstract

Pilots of modern combat aircraft are exposed to the devastating effects of high acceleration forces and unusual orientation. The pilots' ability to perform tasks under these extreme flight conditions must be examined. A centrifuge flight simulator (CFS) for pilot training is designed as a three-degree-of-freedom 3DoF manipulator with rotational axes. Through rotations about these axes, acceleration forces that act on aircraft pilots are simulated. The spatial disorientation trainer (SDT) examines a pilot's ability to recognise unusual orientations, to adapt to unusual positions and to persuade the pilot to believe in the aircraft instruments for orientation and not in his own senses. The SDT is designed as a (4DoF) manipulator with rotational axes. Through rotations about these axes, different orientations can be achieved; different acceleration forces acting on the pilot can also be simulated. In this paper, the acceleration forces and angular velocities that act on the simulator pilot in the CMS and SDT are calculated along with the roll and pitch angles of the gondola for these forces.

Key words: Centrifuge flight simulator · Spatial disorientation trainer · Kinematics · Dynamics · Control algorithm · Robotics

1. Introduction

Modern thrust-vectored jet aircraft have the capability of developing multi-axis accelerations [1,2]. These "agile" aircraft are capable of unconventional flight with high angles of attack, high agile motions in all 3 aircraft axes, rotations around those axes and accelerations of up to 9 g (g is Earth's acceleration), with acceleration rates (jerk) of up to 9 g/s [3,4]. Hence, the destructive effects of the high acceleration forces and the rapid changes of these forces on the pilot's physiology and the ability to perform tasks under these flight conditions must be tested. A human centrifuge is used for the reliable generation of high G onset rates and high levels of sustained G, to test the reactions and the tolerances of the pilots. Here, acceleration force $G=a/g$, $a=(a_n^2+a_t^2+g^2)^{1/2}$ is the magnitude of acceleration acting on the pilot, a_n is normal, and a_t is the tangential acceleration.

The centrifuge (Fig. 1) has the form of a three degree-of-freedom (3DoF) manipulator with rotational axes, where the pilot's head (or chest for some of the training) is considered to be the end-effector [5-10]. The arm rotation around the vertical (planetary) axis is the main motion that achieves the desired acceleration force. CFS must achieve velocity, acceleration and jerk of the pilot through suitable rotations of the centrifuge arm about this axis. The arm carries a gimballed gondola system, with two rotational axes providing pitch and roll capabilities. The roll axis lies in the plane of the arm rotation, perpendicular to the main rotational axis, i.e., in the *x*-axis direction. The pitch (y) axis is perpendicular to the roll axis (Fig. 3). The task of the roll and pitch axes is to direct the acceleration force into the desired direction. It is considered that the pilot's head (chest) is placed in the intersection of the gondola's roll and pitch axes. In this way, the centrifuge produces the transverse G_x, lateral G_y and longitudinal G_z acceleration forces and the roll $\hat{\omega}_x$, pitch $\hat{\omega}_y$ and yaw $\hat{\omega}_z$ angular velocities to simulate the aircraft's acceleration forces and angular velocities.

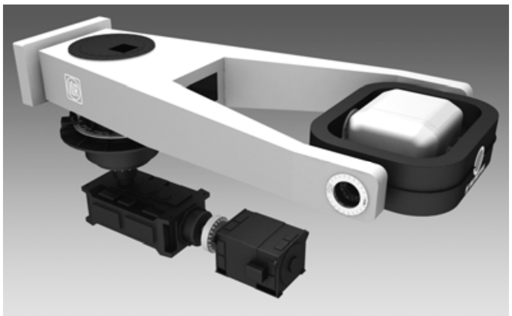

Fig. 1. Centrifuge with 3 degrees of freedom. Fig. 2. SDT with 4 degrees of freedom.

Although the centrifuge is capable of generating acceleration forces of up to 15 g for materials testing purposes, forces that are less than or equal to 9 g are used for pilot training.

Modern jet aircrafts have the capability of achieving different orientations. The SDT examines a pilot's ability to recognise these orientations, to adapt to them and to persuade the pilot to believe only in the aircraft instruments for orientation. The SDT, given in [11], is similar to the CFS, but it has four rotational axes (Fig. 2). Arm rotation around the vertical (i.e., planetary) axis is the primary motion. It carries a gyroscopic gondola system with three rotational axes providing yaw, pitch and roll capabilities. Their task is to achieve any orientation. The yaw axis (z) is parallel with the arm axis. The roll axis lies in the plane of the arm rotation, perpendicular to the main rotational axis (i.e., in the x direction). The pitch (y) axis is perpendicular to the roll axis (Fig. 4).

A forward kinematics analysis of the CFS and SDT is given in Section 2. The calculation of the acceleration forces G_x, G_y and G_z and angular velocities $\hat{\omega}_x$, $\hat{\omega}_y$ and $\hat{\omega}_z$ that act on the simulator pilot and the calculation of the roll and pitch angles of the gondola for the known forces of the CFS and SDT is given in Section 3. The calculation of the angular acceleration of the centrifuge arm $\ddot{q}_1$ is given in Section 4.

2. Forward kinematics of the CFS and SDT

2.1 Forward geometric model of the CFS

This section defines the coordinate frames for the centrifuge links (Fig. 2) and the matrices that determine their relations. The centrifuge links and their coordinate frames are denoted by using the Denavit-Hartenberg convention (D-H) (Fig. 3). The base is denoted by 0, the arm by 1, the roll ring by 2 and the gondola by 3. The arm rotation angle is denoted by q_1=ψ, the roll ring rotation angle by $q_2=\phi$ and the gondola rotation angle (pitch) by $q_3=\theta$. The CFS that was developed as a research result presented in this paper has the following features: arm length a_1=8 m, roll axis rotation range of ±180° and pitch axis rotation range ±360°. The centrifuge base coordinates are denoted by $x_0y_0z_0$, the arm coordinates by $x_1y_1z_1$ (link 1), the roll ring coordinates by $x_2y_2z_2$ (link 2), the gondola coordinates by $x_3y_3z_3$ (link 3) and the pilot coordinates by xyz. Here, $x_3=x$, $y_3=y$ and $z_3=z$. The D-H parameters for the 3-axis CFS components are given in Table 1.

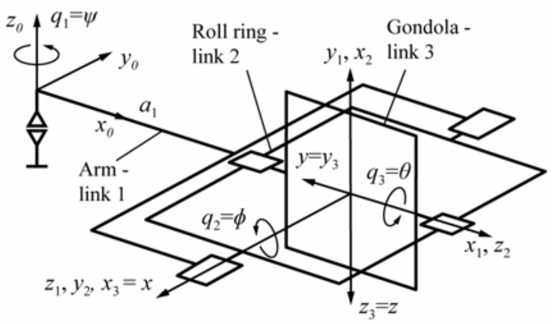

Fig. 3. Coordinate frames of the 3-axis centrifuge links in initial position.

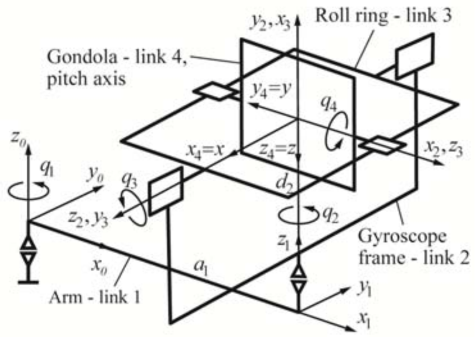

Fig. 4. Coordinate frames of the 4-axis SDT in initial position.

Table 1 D-H parameters for the 3-axis centrifuge links

Link	Variable [º]	a [mm]	d [mm]	α [º]
1	q_1	a_1	0	90
2	q_2 +90	0	0	90
3	q_3+90	0	0	-90

The 4x4 homogenous matrix that transforms the coordinates of a point from frame $x_ny_nz_n$ to frame $x_my_mz_m$ is denoted by ${}^n\mathbf{T}_m$ and from $x_0y_0z_0$ to $x_my_mz_m$ by $\mathbf{T}_m$. ${}^n\mathbf{D}_m$ is a 3x3 orientation matrix, and ${}^n\mathbf{p}_m$ is a 3x1 position vector. This matrix, which describes the relation between one link and the next, is called ${}^{i\text{-}1}\mathbf{A}_i=\mathbf{A}(i\text{-}1,i)$. By using the convenient shorthand notation, $\sin(q_i)=s_i$, $\cos(q_i)=c_i$, the following homogenous matrices for the relation between the centrifuge link coordinate frames are defined to derive the kinematic equations for the machine, as follows:

$$
{}^0\mathbf{A}_1=\mathbf{R}\text{ot}(z_0,\theta_1)\mathbf{T}\text{rans}(x_0,a_1)\mathbf{R}\text{ot}(x_0',90^\circ)=\begin{bmatrix} c_1 & 0 & s_1 & a_1c_1 \\ s_1 & 0 & -c_1 & a_1s_1 \\ 0 & 1 & 0 & 0 \\ 0 & 0 & 0 & 1 \end{bmatrix},\quad
{}^1\mathbf{A}_2=\mathbf{R}\text{ot}(z_1,\theta_2)\mathbf{R}\text{ot}(z_1,90^\circ)\mathbf{R}\text{ot}(x_1',90^\circ)=\begin{bmatrix} -s_2 & 0 & c_2 & 0 \\ c_2 & 0 & s_2 & 0 \\ 0 & 1 & 0 & 0 \\ 0 & 0 & 0 & 1 \end{bmatrix},
$$

$$
{}^2\mathbf{A}_3=\mathbf{R}\text{ot}(z_2,\theta_3)\mathbf{R}\text{ot}(z_2,90^\circ)\mathbf{R}\text{ot}(x_2',-90^\circ)=\begin{bmatrix} -s_3 & 0 & -c_3 & 0 \\ c_3 & 0 & -s_3 & 0 \\ 0 & -1 & 0 & 0 \\ 0 & 0 & 0 & 1 \end{bmatrix} \tag{1}
$$

The forward kinematics that is related to the robot geometry is used to calculate the position and orientation of the links and end-effector (in this case, the pilot's head/chest) with respect to the centrifuge variables q_1, q_2 and q_3. It is determined from the following matrix:

$$\mathbf{T}_3 = {}^0\mathbf{A}_1\, {}^1\mathbf{A}_2\, {}^2\mathbf{A}_3 = \begin{bmatrix} c_1s_2s_3+s_1c_3 & -c_1c_2 & c_1s_2c_3-s_1s_3 & a_1c_1 \\ s_1s_2s_3-c_1c_3 & -s_1c_2 & s_1s_2c_3+c_1s_3 & a_1s_1 \\ -c_2s_3 & -s_2 & -c_2c_3 & 0 \\ 0 & 0 & 0 & 1 \end{bmatrix} \tag{2}$$

2.2 Forward geometric model of the SDT

This section defines the coordinate frames for the SDT links (Fig. 4) and the matrices that determine their relations. The base is denoted by 0, the arm by 1, the gyroscope frame by 2, the roll ring by 3 and the gondola by 4. The arm rotation angle is denoted by q_1, the gyroscope frame rotation angle by q_2, the roll ring rotation angle by $q_3=\phi$ and the gondola rotation angle (i.e., pitch) by $q_4=\theta$. The yaw angle is $\psi=q_1+q_2$. The SDT presented in this paper has the following features: arm length a_1=2.394 m, gyroscope frame length d_2=1.957 m; and q_1, q_2, q_3 and q_4 rotation ranges ±360°. The SDT base coordinates are denoted by x_0, y_0, z_0; the arm coordinates by x_1, y_1, z_1 (link 1); the gyroscope frame by x_2, y_2, z_2 (link 2); the roll ring coordinates by x_3, y_3, z_3 (link 3); the gondola coordinates by x_4, y_4, z_4 (link 4); and the pilot coordinates by x, y, z. It is assumed that $x_4=x$, $y_4=y$ and $z_4=z$. The D-H parameters for the 4-axis SDT links are given in Table 2.

Table 2 D-H parameters for the 4-axis SDT links

Link	Variable [º]	a [mm]	d [mm]	α [º]
1	q_1	a_1	0	0
2	q_2	0	d_2	90
3	q_2+90	0	0	90
4	q_3+90	0	0	-90

The following homogenous matrices for the relation between the SDT links coordinate frames are defined to derive the kinematic equations for the machine as follows:

$${}^0\mathbf{A}_1 = \begin{bmatrix} c_1 & -s_1 & 0 & c_1a_1 \\ s_1 & c_1 & 0 & s_1a_1 \\ 0 & 0 & 1 & 0 \\ 0 & 0 & 0 & 1 \end{bmatrix},\ {}^1\mathbf{A}_2 = \begin{bmatrix} c_2 & 0 & s_2 & 0 \\ s_2 & 0 & -c_2 & 0 \\ 0 & 1 & 0 & d_2 \\ 0 & 0 & 0 & 1 \end{bmatrix},\ {}^2\mathbf{A}_3 = \begin{bmatrix} -s_3 & 0 & c_3 & 0 \\ c_3 & 0 & s_3 & 0 \\ 0 & 1 & 0 & 0 \\ 0 & 0 & 0 & 1 \end{bmatrix},\ {}^3\mathbf{A}_4 = \begin{bmatrix} -s_4 & 0 & -c_4 & 0 \\ c_4 & 0 & -s_4 & 0 \\ 0 & -1 & 0 & 0 \\ 0 & 0 & 0 & 1 \end{bmatrix} \tag{3}$$

Forward kinematics related to robot geometry is used to calculate the position and orientation of the links and end-effector (i.e., the pilot’s head or chest) with respect to the SDT variables q_1, q_2, q_3 and q_4. These are determined from the following matrix:

$$\mathbf{T}_4 = {}^0\mathbf{A}_1\, {}^1\mathbf{A}_2\, {}^2\mathbf{A}_3\, {}^3\mathbf{A}_4 = \begin{bmatrix} c_\psi s_3s_4+s_\psi c_4 & -c_\psi c_3 & c_\psi s_3c_4-s_\psi s_4 & a_1c_1 \\ s_\psi s_3s_4-c_\psi c_4 & -s_\psi c_3 & s_\psi s_3c_4+c_\psi s_4 & a_1s_1 \\ -c_3s_4 & -s_3 & -c_3c_4 & d_2 \\ 0 & 0 & 0 & 1 \end{bmatrix} \tag{4}$$

3. Acceleration force components and roll and pitch link angles

Fig. 5 shows the transverse G_x, lateral G_y and longitudinal G_z acceleration force components acting on the pilot’s head or chest in the CFS or SDT [5,11]. The three main axes of the coordinate frame attached to the human body are the x-axis, which extends from the face to the back; the y-axis which extends from the left to the right side; and the z-axis which extends from the head to the pelvis.

3.1 Calculation of the simulator pilot acceleration force components in the CFS

Fig. 6 shows G_x, G_y and G_z acceleration force G components that act on the pilot's head (chest), coordinate frames, angles, angular velocities and acceleration forces of the centrifuge.

The centrifuge links angular accelerations $\dot{\boldsymbol{\omega}}_{i+1}=\dot{\boldsymbol{\omega}}_i+\mathbf{z}_i\,\ddot{q}_{i+1}+\boldsymbol{\omega}_i\times\mathbf{z}_i\,\dot{q}_{i+1}$, i=1,2,3 are:
$\dot{\boldsymbol{\omega}}_1=[0\ 0\ \ddot{q}_1]^T$, $\dot{\boldsymbol{\omega}}_2=\dot{\boldsymbol{\omega}}_1+[0\ {-1}\ 0]^T\,\ddot{q}_1+[1\ 0\ 0]^T\,\dot{q}_1\dot{q}_2$,
$\dot{\boldsymbol{\omega}}_3=\dot{\boldsymbol{\omega}}_2+[c_2\ 0\ s_2]^T\,\ddot{q}_3+[0\ c_2\ 0]^T\,\dot{q}_1\dot{q}_3+[-c_2\ 0\ c_2]^T\,\dot{q}_2\dot{q}_3$. The linear accelerations
$\dot{\mathbf{v}}_{i+1}=\dot{\mathbf{v}}_i+\dot{\boldsymbol{\omega}}_{i+1}\times\mathbf{p}^*_{i+1}+\boldsymbol{\omega}_{i+1}\times(\boldsymbol{\omega}_{i+1}\times\mathbf{p}^*_{i+1})$, i=1,2,3, where $\mathbf{p}^*_{i+1}=\mathbf{p}_{i+1}-\mathbf{p}_i$, $\mathbf{p}^*_1=[a_1\ 0\ 0]^T$, $\mathbf{p}^*_2=\mathbf{p}^*_3=[0\ 0\ 0]^T$, experienced by the simulator pilot at the intersection point of the roll and pitch axes is:

$$\dot{\mathbf{v}}_1=\dot{\mathbf{v}}_2=\dot{\mathbf{v}}_3=\begin{bmatrix}\dot{v}_{1x} & \dot{v}_{1y} & \dot{v}_{1z}\end{bmatrix}^T=a_1\begin{bmatrix}s_1\dot{\omega}_1+c_1\omega_1^2 & c_1\dot{\omega}_1-s_1\omega_1^2 & 0\end{bmatrix}^T \tag{5}$$

Based on Eq. (6) for q_1=0 and adding the gravitational acceleration g, the orthogonal components G_n, G_t and G_v for the normal (radial), tangential and vertical acceleration force G components, respectively, that are experienced by the simulator pilot are the following:

$$\begin{bmatrix}G_{x0}\\ G_{y0}\\ G_{z0}\end{bmatrix}=\frac{1}{g}\begin{bmatrix}-a_n\\ a_t\\ -g\end{bmatrix}=\begin{bmatrix}a_1\omega_1^2/g\\ -a_1\dot{\omega}_1/g\\ -1\end{bmatrix}=\begin{bmatrix}G_n\\ -G_t\\ -G_v\end{bmatrix} \tag{6}$$

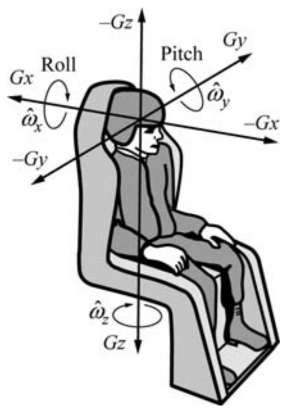

Fig. 5. The transverse, lateral and longitudinal acceleration force components G_x, G_y and G_z which act on the pilot in the simulator.

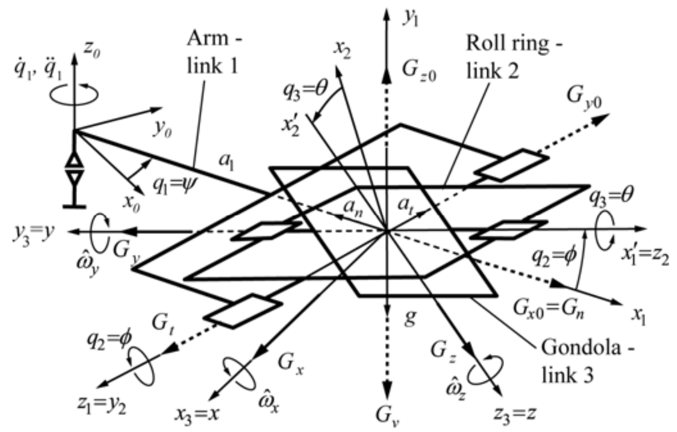

Fig. 6. The transverse, lateral and longitudinal acceleration force components G_x, G_y and G_z, which act on the pilot in the CFS.

The link angles $q_2=\phi$ and $q_3=\theta$ and the angular velocity $\dot{q}_1$ of the arm define the orthogonal components G_x, G_y and G_z of the resultant vector $\mathbf{G}$ that are experienced by the simulator pilot. Based on Eqs. (2) and (6), the resultant vector $\mathbf{G}$ is:

$$\mathbf{G}=\begin{bmatrix}G_x & G_y & G_z\end{bmatrix}^T=\mathbf{D}_3^{-1}\begin{bmatrix}G_{x0} & G_{y0} & G_{z0}\end{bmatrix}^T \tag{7}$$

$$G_x=s_3(G_{x0}s_2+c_2)-G_{y0}c_3 \tag{8}$$

$$G_y=-G_{x0}c_2+s_2 \tag{9}$$

$$G_z=c_3(G_{x0}s_2+c_2)+G_{y0}s_3 \tag{10}$$

Angles $q_1=\psi$, $q_2=\phi$ and $q_3=\theta$ and their derivatives define the roll, pitch and yaw angular velocities of $\hat{\omega}_x$, $\hat{\omega}_y$ and $\hat{\omega}_z$, which are experienced by the simulator pilot; they are given in the following equations (for q_1=0):

$$\hat{\boldsymbol{\omega}} = \begin{bmatrix} \hat{\omega}_x & \hat{\omega}_y & \hat{\omega}_z \end{bmatrix}^T = \mathbf{D}_3^{-1}\boldsymbol{\omega}_3 = \mathbf{D}_3^{-1}\begin{bmatrix} c_\phi \dot{q}_\theta & -\dot{q}_\phi & \dot{q}_\psi + s_\phi \dot{q}_\theta \end{bmatrix}^T \tag{11}$$

$$\hat{\omega}_x = \dot{\phi} c_\theta - \omega_1 c_\phi s_\theta \tag{12}$$

$$\hat{\omega}_y = -\dot{\theta} - \omega_1 s_\phi \tag{13}$$

$$\hat{\omega}_z = -\dot{\phi} s_\theta - \omega_1 c_\phi c_\theta \tag{14}$$

3.2 Calculation of the centrifuge roll and pitch angles

The centrifuge roll angle is calculated by Eq. (9), which uses the given lateral force G_y, in the following way:

$$q_2 = \phi = \operatorname{atan2}(G_{x0} + G_y(1 - G_y^2 + G_{x0}^2)^{1/2}, 1 - G_y^2) \tag{15}$$

If $G_y < 0$ and $G_y^2 > 1$, then $q_2 = q_2 + \pi$.

The function atan2 is the arctangent function with two arguments which is used in a variety of computer languages (C++, Java, Matlab).
The roll angle can be calculated only if $G_{x0}^2 + 1 \geq G_y^2$. Otherwise, it is not possible to achieve the given lateral force G_y. For G_y=0, Eq. (15) yields:

$$q_2 = \phi = \operatorname{atan2}(G_{x0}, 1) \tag{16}$$

Eqs. (8) and (10) show that it is not possible to achieve both of the given G_x and G_z forces, even when they are in the allowed ranges. As a result, the centrifuge pitch angle is calculated by Eq. (8), using the given transverse force G_x, or by Eq. (10), using the given longitudinal G_z force. Eq. (8) yields:

$$q_3 = \theta = \operatorname{atan2}(G_{y0} b + G_x(b^2 + G_{y0}^2 - G_x^2)^{1/2}, b^2 - G_x^2) \tag{17}$$

where $b = G_{x0} s_2 + c_2$. If $b^2 + G_{y0}^2 < G_x^2$, then it is not possible to achieve the given transverse force G_x. For G_x=0, Eq. (16) yields:

$$q_3 = \theta = \operatorname{atan2}(G_{y0}, b) \tag{18}$$

Eq. (10) yields the following:

$$q_3 = \theta = \operatorname{atan2}(G_{y0} d - G_z(b^2 + G_{y0}^2 - G_z^2)^{1/2}, G_z^2 - G_{y0}^2) \tag{19}$$

If $G_z < 0$ and $G_z^2 > G_{y0}^2$, then is $q_3 = q_3 - \pi$. If $b^2 + G_{y0}^2 < G_z^2$, then it is not possible to achieve the given longitudinal G_z force. Basic pilot training implies that G_z=G (G_x=0 and G_y=0). Consequently, the roll and pitch angles are given by Eqs. (16) and (18).

3.3. Calculation of the pilot SDT acceleration forces

Fig. 7 shows the coordinate frames, angles, angular velocities and acceleration forces of the SDT. The linear acceleration experienced by the simulator pilot at the intersection point of the roll and pitch axes is the same as by CFS, Eq. (5). The same is for the acceleration components

Based on this equation, for q_1=q_2=0 and a gravitational acceleration g, the acceleration force components G_n, G_t and G_v are the same as in CFS, Eq. (6).

Angles q_2, q_3 and q_4, the angular velocity ω_1, and the angular acceleration $\dot{\omega}_1$ of the arm define the orthogonal components G_x, G_y and G_z of the resultant vector **G** experienced by the simulator pilot. Based on Eqs. (4) and (6), the resultant vector **G** is:

$$\mathbf{G} = \begin{bmatrix} G_x & G_y & G_z \end{bmatrix}^T = \mathbf{D}_4^{-1} \begin{bmatrix} G_{x0} & G_{y0} & G_{z0} \end{bmatrix}^T \tag{20}$$

$$G_x = (c_2 s_3 s_4 + s_2 c_4) G_{x0} + (s_2 s_3 s_4 - c_2 c_4) G_{y0} + c_3 s_4 \tag{21}$$

$$G_y = -c_3 (c_2 G_{x0} + s_2 G_{y0}) + s_3 \tag{22}$$

$$G_z = (c_2 s_3 c_4 - s_2 s_4) G_{x0} + (s_2 s_3 c_4 + c_2 s_4) G_{y0} + c_3 c_4 \tag{23}$$

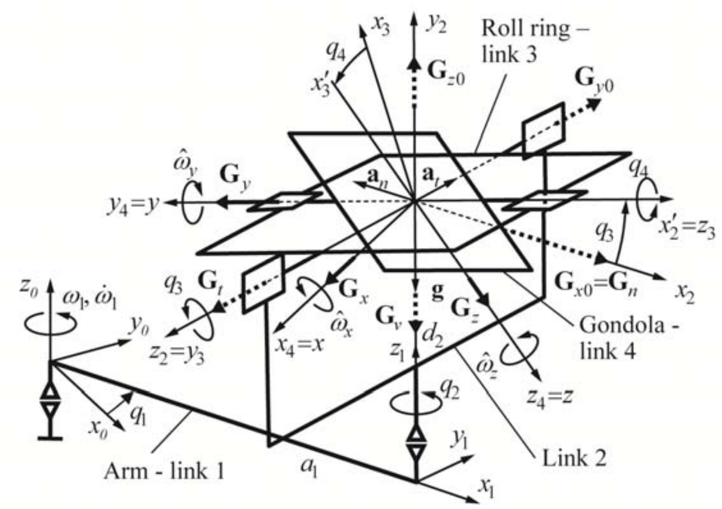

Fig. 7. Coordinate frames, angles, angular velocities and acceleration forces of the 4-axis SDT.

Angles q_3=ϕ and q_4=θ and their derivatives, and the derivatives of the angles q_1 and q_2 define the roll, pitch, and yaw angular velocities $\hat{\omega}_x$, $\hat{\omega}_y$ and $\hat{\omega}_z$ experienced by the simulator pilot. These are given in the following equations for q_1=0:

$$\hat{\boldsymbol{\omega}} = \begin{bmatrix} \hat{\omega}_x & \hat{\omega}_y & \hat{\omega}_z \end{bmatrix}^T = \mathbf{D}_4^{-1} \boldsymbol{\omega}_4 = \mathbf{D}_4^{-1} \begin{bmatrix} s_\psi \dot{q}_3 + c_\psi c_3 \dot{q}_4 & -c_\psi \dot{q}_3 + s_\psi c_3 \dot{q}_4 & \dot{q}_\psi + s_3 \dot{q}_4 \end{bmatrix}^T \tag{24}$$

$$\hat{\omega}_x = c_4 \dot{q}_3 - c_3 s_4 \dot{q}_\psi \tag{25}$$

$$\hat{\omega}_y = -\dot{q}_4 - s_3 \dot{q}_\psi \tag{26}$$

$$\hat{\omega}_z = -s_4 \dot{q}_3 - c_3 c_4 \dot{q}_\psi \tag{27}$$

3.2. Calculation of the roll and pitch angles of the SDT

The calculation of the roll and pitch angles of the gondola for the known acceleration forces are shown below. These angles can be calculated for the known angle q_2. The roll angle is calculated by Eq. (22) using the given lateral force G_y, in the following way:

$$q_3 = \phi = \text{atan}\,2(p_1 + G_y (1 - G_y^2 + p_1^2)^{1/2}, 1 - G_y^2) \tag{28}$$

where $p_1 = c_2 G_{x0} + s_2 G_{y0}$. If $G_y < 0$ and $G_y^2 > 1$, then is $q_3 = q_3 + \pi$.

If $p_1 + G_y(1 - G_y^2 + p_1^2)^{1/2} > 0$ and $G_y = 1$, then $q_3 = 90°$,

if $p_1 + G_y(1 - G_y^2 + p_1^2)^{1/2} < 0$ and $G_y = 1$, then $q_3 = -90°$, and

if $p_1 + G_y(1 - G_y^2 + p_1^2)^{1/2} = 0$ and $G_y = 1$, then q_3 is undefined.

The roll angle can be calculated only if $p_1^2 + 1 \geq G_y^2$ is satisfied; otherwise it is not possible to achieve the given lateral force G_y. For G_y=0, Eq. (28) yields:

$$q_3 = \phi = \operatorname{atan2}(p_1, 1) \tag{29}$$

Eqs. (21) and (23) show that it is not possible to achieve both of the given G_x and G_z forces, even when they are in the allowed ranges. As a result, the SDT pitch angle is calculated by Eq. (21), using the given transverse force G_x, or by Eq. (26), using the given longitudinal G_z force. Eq. (21) yields:

$$q_4 = \theta = \operatorname{atan2}(G_x(p_2^2 + p_3^2 - G_x^2)^{1/2} - p_2 p_3,\ p_2^2 - G_x^2) \tag{30}$$

where $p_2 = c_2 s_3 G_{x0} + s_2 s_3 G_{y0} + c_3$, $p_3 = s_2 G_{x0} - c_2 G_{y0}$.

If $G_x(p_2^2 + p_3^2 - G_x^2)^{1/2} - p_2 p_3 > 0$ and $G_x = p_2$, then $q_4 = 90°$,

if $G_x(p_2^2 + p_3^2 - G_x^2)^{1/2} - p_2 p_3 < 0$ and $G_x = p_2$, then $q_4 = -90°$, and

if $G_x(p_2^2 + p_3^2 - G_x^2)^{1/2} - p_2 p_3 = 0$ and $G_x = p_2$, then q_4 is undefined.

If $p_2^2 + p_3^2 < G_x^2$, then it is not possible to achieve the given transverse force G_x. For G_x=0, Eq. (30) yields:

$$q_4 = \theta = \operatorname{atan2}(-p_3, p_2) \tag{31}$$

Eq. (26) yields the following:

$$q_4 = \theta = \operatorname{atan2}(p_2 p_3 - G_z(p_2^2 + p_3^2 - G_z^2)^{1/2},\ p_3^2 - G_z^2) \tag{32}$$

If $G_z < 0$ and $G_z^2 < p_3^2$, then is $q_4 = q_4 - \pi$. If $p_2^2 + p_3^2 < G_z^2$, then it is not possible to achieve the given longitudinal G_z force.

4. Calculation of the angular acceleration $\ddot{q}_1$

Eq. (6) gives the resulting force that is experienced by the simulator pilot at the intersection point of the roll and pitch axes (for q_1=0) as a function of the angular velocity and acceleration of the centrifuge arm, which is:

$$G = (G_{x0}^2 + G_{y0}^2 + G_{z0}^2)^{1/2} = (a_n^2 + a_t^2 + g^2)^{1/2}/g = [a_1^2(\dot{q}_1^4 + \ddot{q}_1^2) + g^2]^{1/2}/g \tag{33}$$

According to the requirement that the increase in the acceleration force G should be constant and equal to n, the following is valid:

$\dfrac{dG}{dt} = \dfrac{d}{dt}\dfrac{1}{g}[a_1^2(\dot{q}_1^4 + \ddot{q}_1^2) + g^2]^{1/2} = n$, which yields $d([a_1^2(\dot{q}_1^4 + \ddot{q}_1^2) + g^2]^{1/2}) = n\,g\,dt$. If we assign the resulting acceleration with $a= G\,g$, then the previous equation will be:

$$da = d([a_1^2(\dot{q}_1^4 + \ddot{q}_1^2) + g^2]^{1/2}) = n\,g\,dt \tag{34}$$

The previous differential equation does not have a solution in the general case.

In each interpolation period, the robot controller determines the angular velocities of each motor link. An interpolation period of Δt=0.005 s is adopted here. During this period, the servo system of the controller compares (every 0.001 s) the given and achieved motor rotor positions and corrects rotor angular velocities. Based on these observations, an approximated solution from Eq. (34) using a discretisation technique is obtained in the following manner. This approach allows us to solve this differential equation for each interpolation period Δt, which simplifies the solution. For the given rate of change of acceleration $\Delta a/\Delta t = ng$, the acceleration *a* will first be calculated on the basis of this acceleration in the previous interpolation period, a_{prev}, in the following way:

$$a = a_{prev} + \Delta a\ ,\ \ \Delta a = n\, g\, \Delta t \tag{35}$$

If we assign the angular velocity of the centrifuge arm in the previous interpolation period with $\dot{q}_{1prev}$, we obtain:

$$\dot{q}_1 = \dot{q}_{1prev} + \ddot{q}_1\, \Delta t \tag{36}$$

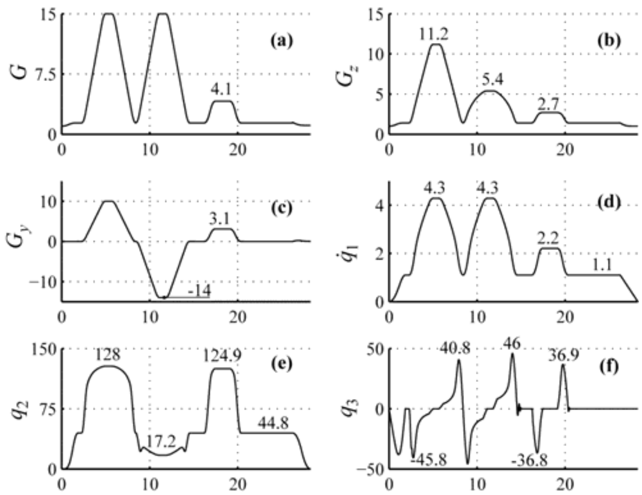

Fig. 8. Example of the kinematics parameters of the centrifuge motion: (a) *G*, (b) G_z, (c) G_y, (d) $\dot{q}_1$ [s^{-1}], (e) $q_2=\phi$ [°], (f) $q_3=\theta$ [°].

If we substitute $\dot{q}_1$ calculated in this manner into the equation $a^2 = a_1^2\dot{q}_1^4 + a_1^2\ddot{q}_1^2 + g^2$ and neglect the terms with Δt^3 and Δt^4, the following equation for calculating the centrifuge arm acceleration is obtained:

$$\ddot{q}_1 = \frac{-2\dot{q}_{1prev}^3\, \Delta t + [(1+6\dot{q}_{1prev}^2 \Delta t^2)(a^2-g^2)/a_1^2 - 2\dot{q}_{1prev}^6 \Delta t^2 - \dot{q}_{1prev}^4]^{1/2}}{1+6\dot{q}_{1prev}^2 \Delta t^2} \tag{37}$$

The previous equation is valid for the movement that has a positive acceleration onset. For the movement that has a negative acceleration onset, the discriminant $(1+6\dot{q}_{1prev}^2 \Delta t^2)(a^2-g^2)/a_1^2 - 2\dot{q}_{1prev}^6 \Delta t^2 - \dot{q}_{1prev}^4$ is mostly negative, which means that this equation cannot be used directly. In that case, a simple solution is used, in which the values of $\ddot{q}_1$ for the positive acceleration onset *n* of the same magnitude are reversed.

In [12], Eq. (34) is solved, for every interpolation period, using principle given in Eq. (35) as well. Solution is obtained in the form of Jacobi elliptic integrals.

Fig. 8 shows kinematics parameters of an example of the centrifuge motion program obtained with the suggested algorithms.

3. Conclusions

The calculation of the transverse G_x, lateral G_y and longitudinal G_z acceleration forces and angular velocities experienced by the simulator pilot in the gondola and the roll and pitch angles of the gondola of the CFS and SDT for the known acceleration forces is given in this paper.

The method for the calculation the angular acceleration $\ddot{q}_1$ that gives the constant increase in the acceleration force G is also given in the paper.

Acknowledgments This research is supported by the Ministry of Education, Science and Technological Development of Serbia under the project “Development of devices for pilot training and dynamic simulation of modern fighter planes flights: 3DoF centrifuge and 4DoF spatial disorientation trainer” (2011-2016), no. 35023.

References

[1] Albery WB., *Current and Future Trends in Human Centrifuge Development*, SAFE Journal, 29, 2, September 1999.

[2] Albery WB., *Acceleration in Other Axes Affects +G_z Tolerance: Dynamic Centrifuge Simulation of Agile Flight*, Aviat Space Environ Med. 2004 Jan;75(1): 1-6.

[3] Schot SH. Jerk: the time rate of change acceleration. American J. of Physics 1978; 46(11): 1090–4.

[4] Gallardo-Alvarado J., *Jerk analysis of a six-degrees-of-freedom three-legged parallel manipulator*, Robotics and Computer-Integrated Manufacturing 2012; 28: 220–226.

[5] Kvrgic, V., Vidakovic, J., Lutovac, M., Ferenc, G., Cvijanovic, V., *A control algorithm for a centrifuge motion simulator*. Robotics and Computer-Integrated Manufacturing (2014) 30(4): 399–412.

[6] Lutovac M, Kvrgic V, Ferenc G, Dimic Z, Vidakovic J, *3D simulator for human centrifuge motion testing and verification*, 2nd Mediterranean Conf. on Embedded Computing MECO 2013, pp. 160-163.

[7] Crosbie RJ., *Dynamic flight simulator control system*, United States Patent, Number 4,751,662, Jun.14, 1988.

[8] Crosbie RJ, Kiefer DA., *Controlling the Human Centrifuge as a Force and Motion Platform for the Dynamic Flight Simulator Technologies*, Proceedings of the AIAA Flight Simulation Conference, St Louis, MO, AIAA Paper, 37-45, 1985.

[9] Vidaković, J., Lazarević, M., Kvrgić, V., Dančuo, Z., Ferenc, G., *Advanced Quaternion Forward Kinematics Algorithm Including Overview of Different Methods for Robot Kinematics*, FME Transactions, vol. 42, no. 3 (2014) pp. 189-198.

[10] Vidaković, J., Kvrgić, V., Ferenc, G., Dančuo, Z., Lazarevic, M., *Kinematic and dynamic model of the human centrifuge*, Proc. of the Serbian Society of Mechanics SSM Fourth Serbian Congress on Theoretical and Applied Mechanics, pp. 627-632 (2013).

[11] Kvrgic, V., Visnjic, Z., Cvijanovic, V., Divnic, D., Mitrovic, S., *Dynamics and control of a spatial disorientation trainer*, Robotics and Computer-Integrated Manufacturing (2015) 35: 104–125.

[12] Vidakovic J, Ferenc G, Lutovac M, Kvrgic V., *Development and implementation of an algorithm for calculating angular velocity of main arm of human centrifuge Source*, 15th I. Power Electronics and Motion Conf., EPE-ECCE 2012 Europe Congress, pp.DS2a.17, 2012.